ESTIMATING THE EFFECT OF SHEAR STRENGTH INCREMENT DUE TO ROOT ON THE STABILITY OF MAKINO BAMBOO FOREST SLOPELAND

Der-Guey Lin[1], Wen-Tsung Liu[2], and Shin-Hwei Lin[3]

ABSTRACT

Due to the benefit of agriculture economics, Makino bamboo (Phyllostachys Makinoi Hayata) was chosen as one of the most important species for forest plantation during 1980's in Taiwan to control slopeland erosion and landslides. However, after the Chi-Chi (or 921) earthquake in 1999, shallow landslides frequently occurred at the Makino bamboo forest slopeland during typhoons. To investigate the shear strength characteristics of the soil-root system of Makino bamboo forest, a 3-D numerical root model consisted of a reverse *T*-shape rhizome roots and limit hair roots was developed according to the actual root morphology, and successfully applied to the numerical simulation of the in-situ pull-out tests of soil-root system. Meanwhile, the ultimate pull-out resistance can be well correlated with the growth age, diameter at breast height and soil water content. Using the identical 3-D numerical root model to the pull-out test, a series of numerical simulations of direct shear tests were implemented and the shear strength increment of soil mass due to roots was estimated. Subsequently, a mechanical conversion model with simple mathematical form, which enables a direct transformation of the observed ultimate pull-out resistance of 2.28 to 6.12 kN into the shear strength increment of 2.83 to 36.45 kPa due to roots was proposed. The conversion model offered a convenient way to estimate the reinforcement effect of the Makino bamboo root system required for the 3-D slope stability analyses. For a Makino bamboo forest slopeland with slope angle varies from 20° to 50°, the maximum increment of factor safety due to the reinforcement effect of Makino bamboo root system approximates 4.6% and the contribution of the root system to the stabilization of slopeland is not as significant as expected. Conclusively, according to the field observations, it can be inferred that the tension cracks widespread over the slopeland due to the wind loading on Bamboo culms during typhoons and the sequential infiltration of rainwater into cracks are the main factors responsible for the collapse failure of slopeland.

Key words: Makino bamboo, soil-root system, ultimate pull-out resistance, shear strength increment.

1. INTRODUCTION

Because of the benefit of agriculture economics and the suitability of vegetative reproduction for the local environment, Makino bamboo was chosen for forest plantation by public agencies during 1980′s in Taiwan. As a consequence, Makino bamboo has the greatest accumulative population among the several main species of bamboo due to the numerous plantations by peasants in that duration (Yang and Huang 1981). Before the Chi-Chi (or 921) earthquake in 1999, Makino bamboo was considered as an appropriate species of forest plantations with contribution to the erosion control and landslide prevention of the slopeland of watershed in Taiwan (Chen *et al*. 2005). However, after the earthquake, shallow landslides of Makino bamboo forest slopeland (see Fig. 1) became very common during typhoons and this implies the policy of using Makino bamboo for the long-term forest plantations might need to be further inspected.

Manuscript received March 8, 2011; revised March 30, 2011; accepted March 30, 2011.

[1] Professor, Department of Soil and Water Conservation, National Chung-Hsing University, Taichung, Taiwan.

[2] Associate Professor, Department of Civil Engineering, Kao-Yuan University, Kaohsiung, Taiwan.

[3] Professor (corresponding author), Department of Soil and Water Conservation, National Chung-Hsing University, Taichung, Taiwan (e-mail: shlin@dragon.nchu.edu.tw).

A large amount of direct shear tests and formulations of mechanical models of soil-root systems were carried out to quantify the reinforcement effect of root systems on soil mass (Waldron 1977; Waldron and Dakessian 1981; Wu *et al*. 1979, 1988a and 1998b; Abe and Ziemer 1991; Operstein and Frydman 2000; Cazzuffi and Crippa 2005). Various soil-root interaction models were also proposed to evaluate the contribution of roots to shear strength and comprehensive reviews can be found in many works (Coppin and Richards 1990; Morgan and Rickson 1995; Gray and Sotir 1996; Wu *et al*. 2004). Abe (1991) estimated the reinforced shear resistance of roots through the pull-out resistance of roots. Operstein and Frydman (2000) carried out 43 pull-out tests to measure the vertical pull-out load of Alfalfa roots from a waste chalky fill with varying stone content. Conclusively, the morphology of plant roots in soil stratum dominates the anchorage of plants to resist the uprooting force (Stokes *et al*. 1996; Ennos 1990 and 1991).

Dupuy *et al*. (2005a) used the density-based approach to model the architecture of roots and investigated the anchorage of roots by 2-D numerical analyses. Operstein and Frydman (2001) simulated the direct shear behavior of cylindrical samples with and without roots using a 2-D finite difference plane strain numerical scheme to examine the reinforcement effect of roots. Dupuy L. *et al*. (2005b, 2005c and 2007) also investigated the influence of root morphology and soil type on the uprooting resistance and overturning resistance of trees through 2-D and 3-D numerical modeling.

(a) Typical failure mode of Makino bamboo forest slopeland

(b) Makino bamboo root system with shallow rooting depth

Fig. 1 Shallow landslides frequently occurred at Makino bamboo forest slopeland during typhoon

Although many soil-root interaction mechanical models and pull-out test of roots had been proposed to evaluate the shear strength increment due to roots, none of them can directly correlate the shear strength increment with the pull-out resistance of roots.

In the past, the relevant studies of Makino bamboo were mainly concentrated on its growth characteristics, biomass investigations, population distributions, and utilizations (Liu and Ren 1971; Lee 1983) rather than on their mechanical functions of root system. Stokes *et al*. (2007) performed a systematic uprooting tests and measured the plant morphological characteristics to quantify the anchorage of the root system of big node bamboo and indicated that the root system is contributes little to slope stability. However, the quantitative contribution of the root system of the bamboo to the shear strength increment of soil mass is still not available and needs more surveys.

In this study, a series of in-situ pull-out tests were carried out to evaluate the anchorage resistance of Makino bamboo root systems. In addition, a 3-D numerical model of a Makino bamboo soil-root system with optimum geometry configuration was established for the 3-D finite element numerical simulations of in-situ pull-out tests. Simultaneously, the identical 3-D numerical model to the pull-out test was repeatedly used for the simulation of the direct shear test to estimate the shear strength increment of soil mass due to roots. A mechanical conversion model, which enables a direct transformation of the ultimate pull-out resistance into the shear strength increment of the Makino bamboo soil-root system, was proposed and used for a series of 3-D stability analyses of the Makino Bamboo forest slopeland in watersheds.

2. MATERIALS AND METHOD

2.1 Field Investigations of Makino Bamboo Forest

The study site was located at the mileage 27 km of Pei-Heng Highway in Da-Xi forest land No. 167, Fu-Hsing Township, Tao-yuan County, Taiwan and attributed to the watershed of the Shi-Men Reservoir as shown in Fig. 2. The elevation of the area is about 1,752 m and characterized by mild slopes with an average gradient of 20°. The major soil types are silty clay or clay with

low plasticity. The climate of the area is subtropical with high humidity, annual average relative humidity of 83%, annual mean temperature of 24.7°C in summer and 14.6°C in winter. In addition, average annual precipitation ranges from 2,260 to 2,680 mm with large percentage from May to September.

2.2 Physiological and Growth Characteristics of the Root System

Makino bamboo forest was widespread over the slopeland of the watershed with an elevations ranging from 10 to 1,550 m in the central and south parts of Taiwan and a total distribution area approximating 44,000 hectares. According to the biomass investigations from ten sampling sites by Lin *et al*. (2009), the stand density of Makino bamboo forest ranges from 10,200 to 16,500 trees/ha.

The bamboo culms are connected each other through a network-like shape of laterally running root system called rhizomes (or rhizome roots). In the loose soil stratum of bare land or landslide areas, the length of new growing roots can reach 30 m per year. The rooting depth of Makino bamboo is shallow (< 0.8 m) and the root density decreases with the increasing depth of the soil layer.

The culms and root system of Makino bamboo have a life cycle of about 10 years and the bamboo shows a very high germination and propagation rates in its growth age between 3 and 5 years. The diameter at breast height (*DBH*) of Makino bamboo directly measured from the 10 sampling sites ranges from 50 to 60 mm and the growth age was estimated about 1 to 3 years old by the facial color of the bamboo stand. The growth conditions of Makino bamboo forest investigated by Lin *et al*. (2009) are summarized in Table 1.

2.3 Morphology of the Root System

Four test pits were excavated to survey the morphology of the Makino bamboo root system as shown in Figs. 3(a) and 3(b). Makino bamboo is monopodial with a laterally running type of root system (called rhizomes or rhizome roots) and individual culms emerge from the rhizomes at different distances.

The root system of Makino bamboo can be considered as a reverse *T*-shape rhizome roots system (vertical rhizome roots + lateral rhizome roots) and plenty of hair roots as presented in Fig. 3(c). The vertical rhizome roots extend downward to a depth from 0.1 to 0.3 m (= L_{VR}) and the lateral rhizome roots grow laterally to a range from 0.4 to 0.5 m (= L_{LR}). The diameter of both roots ranges from 13 to 25 mm (= d_R). In addition, the hair root sprouts from the knot of the lateral rhizome roots and spreads widely over the soil layers nearby the ground surface. The diameter of hair root ranges from 10 to 20 mm (= d_H) and the stretching length can reach 0.6 m (= L_{VH} or L_{LH}). The biomass of the hair root decreases with the increasing depth. In general, the Makino bamboo root system can grow and extend downward to a depth from 0.7 to 1.0 m from the ground surface. Figure 3(d) illustrates a small Makino bamboo community consisted of 11 bamboo culms with 63 rhizome roots.

Table 1 Growth conditions of Makino bamboo in the field site

Da-Xi No. 167 forest land, Fu-hsing Township, Tao-yuan County, Taiwan m.s.l. (mean sea level) = 470 m				
Stand density (tree/ha)	Average diameter at breast height DBH (mm)	Average stand total height (m)	Average stand height under crown (m)	Total weight of stand above ground surface (kN/ha)
15800±2651	54.0±12.0	10.8±1.0	8.1±1.6	1527.9±152.0

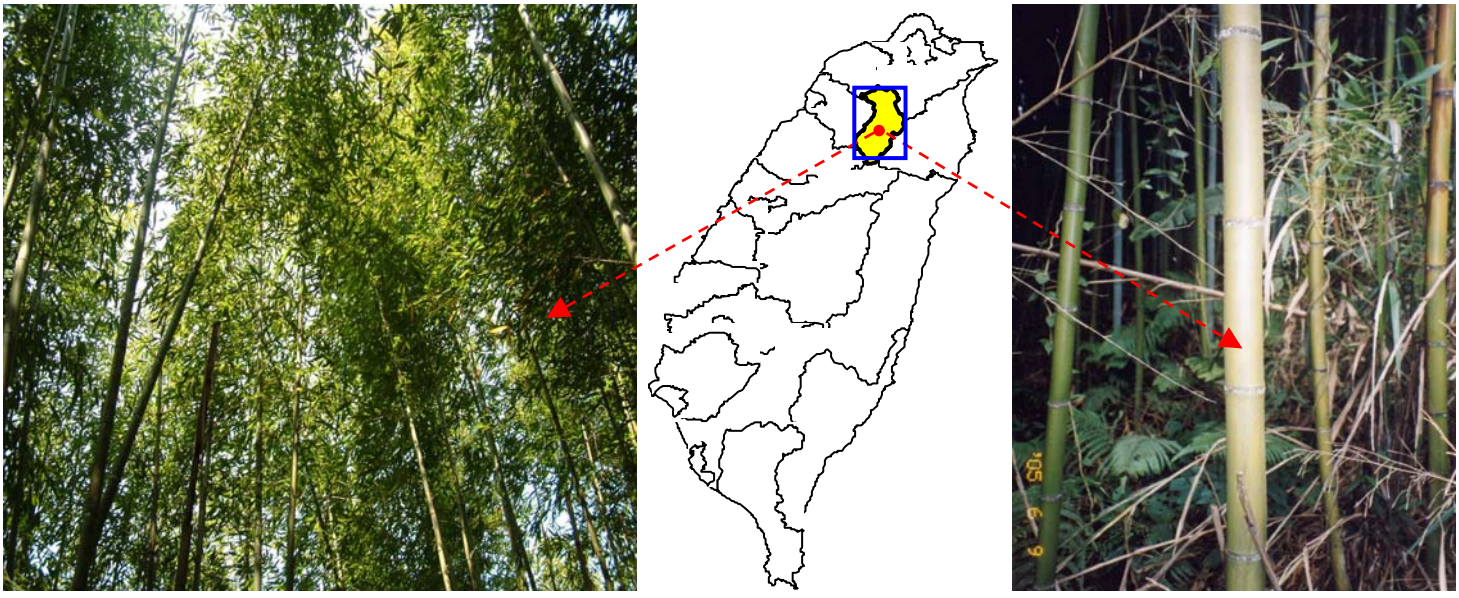

(a) Makino bamboo with high culm (b) Location of Makino bamboo forest (c) Culm color of Makino bamboo varied with growth age

Fig. 2 The study site of Makino bamboo forest located at the watershed of the Shi-Men Reservoir in Taiwan

2.4 Laboratory Strength Tests

Strength Tests of Root Material

The live cutting rhizome roots were packed into plastic bag and sealed immediately after the sampling in the field. To keep the roots fresh, the root specimens were stored in refrigerator prior to testing. On the other hand, without using oven dry, the withered roots dry naturally in the field called dry dead roots were also collected for strength tests. There totally 20 and 5 tensile tests were carried out in the laboratory for live cutting roots and dry dead roots respectively and another 5 shear tests were performed for live cutting roots. The length of root ranges from 400 to 500 mm for tensile test and from 200 to 250 mm for shear tests. The strength tests were carried out by strain control with a loading speed of 10 mm/min. using the universal test machine with capacity of 1MN.

Direct Shear Tests of In-situ Soil Material

There totally nine pull-out tests were performed and the relevant testing results are summarized in Table 2. In addition, the in-situ soil material was classified into the silty clay (*CL*) or silty soil (*ML*) according to the United Soil Classification System (USCS). Three groups of soil specimens (soil *No-A*) sampled from the field site of pull-out test were used for laboratory direct shear tests to determine the shear strength of soil material. The average total (or moisture) unit weight of soil specimens was 18.5 kN/m^3.

2.5 In-situ Pull-out Tests

The layout of the pull-out equipment is illustrated in Fig. 4. The load cell (capacity: 50 kN) was firstly connected with the pull-out loading recorder (equipment type: SMD-10A) and constant rate pull-out unit (rate adjustable from 0.157 to 4.993 mm/min); and finally mounted on the portable triangular frame. The pull-out loading recorder connected with the computer enabled a data acquisition of the pull-out resistance and pull-out displacement. To save time and promote the testing efficiency in the bamboo forest, nine sets in total of the pull-out tests (No. *T*1 ~ *T*9) as shown in Table 2 were carried out under a maximum pull-out rate of 4.993 mm/min and the growth age of the bamboo for the test ranged from 1 yr to 3 yrs.

2.6 Numerical Model of Pull-out Test

In this study, both the numerical modeling of pull-out test and direct shear test were performed using the finite element program of Plaxis-3D Foundation (2008). Unlike the 2-D plane strain model, the 3-D model enables a more realistic simulation on the stiffness and the configuration of the root system. The numerical model with dimensions of 3 × 3 × 3 m (length × width × height) were adopted to minimize the boundary effect on the numerical solutions of the pull-out test carried out at the central area of the model and the geometry boundaries were specified as being in a fully constrained condition as shown in Fig. 5.

According to the root morphology in Figs. 3(a) ~ 3(d), the geometry of the root system were approximated by two components: (1) The reverse *T*-shape rhizome roots: Grows and extends downward to a depth of L_{VT} = 0.15 m beneath the surface of the ground and laterally stretches to a length of L_{LT} = 0.5 m (2 × 0.25 m) with an average diameter of 19 mm (= d_R); (2) The hair root: The lengths of the vertical hair root L_{VH} = 0.5 m and lateral hair root L_{LH} = 0.25 and 0.35 m were used for the parametric study. The average diameter of the hair root is 1.5 mm (= d_H).

Figure 6 illustrates the detail of the 3-D numerical root model. Adjusting for the length and the number of layers of lateral hair root, four types (*S*1 ~ *S*4) of numerical root model as tabulated in Table 3 were established for numerical experiments. In which, all types of root models contained the reverse *T*-shape rhizome root except that the sample *S*1 didn't include the vertical hair root and lateral hair root.

Input Material Model Parameters of Pull-out Test

In this study, the soil material was simulated by the soil element with perfectly elastic plastic model (or Mohr-Coulomb model). The shear strength parameters of soil *No-A*, namely, the cohesion, c = 24.0 kPa, and friction angle, ϕ =15.6°, determined from the laboratory direct shear tests were used for the numerical simulation of pull-out tests. In addition, the required model parameters consisted of the Young's modulus of soil material, E = 2000 kPa, Poisson's ratio, ν = 0.30, and the dilation angle, ψ = 0 and they were all specified according to the engineering characteristics of low plasticity silty clay (Plaxis-3D Foundation, 2008).

In addition to the model parameters, the relative displacement at the soil-root interface during the pull-out test was modeled by two strength parameters c_{int} and ϕ_{int}. At the interface, the c_{int} and ϕ_{int} were given by: c_{int} (= R_{int} × c) and ϕ_{int} (= R_{int} × [$\tan^{-1}(\tan\phi)$]), in which, the strength reduction factor R_{int} = 0.5 was adopted considering the lower overburden pressure of soil-root system.

Table 2 In-situ pull-out tests of Makino bamboo soil-root system

Testing No.	Growth age (yr)	*DBH* (mm)	δ_p (mm)	P_u (kN)	n_b	w (%)
*T*1	1	35	87	2.28	1	12
*T*2	1	40	84	2.58	1	18
*T*3	1	45	98	4.08	2	10
*T*4*	2	50	181	6.12	3	7
*T*5*	2	55	112	4.99	2	13
*T*6*	2	55	99	5.88	2	9
*T*7	3	65	131	5.67	3	13
*T*8*	3	58	190	5.36	3	12
*T*9	3	70	136	5.91	4	15

DBH = diameter at breast height; δ_p = measured pull-out displacement at ultimate pull-out resistance; P_u = measured ultimate pull-out resistance; n_b = number of tap root breakage; w = water content of soil mass; *good similarity in P_u ~ δ_p testing curves and used for the comparisons with numerical results

(a) Before culms cutting

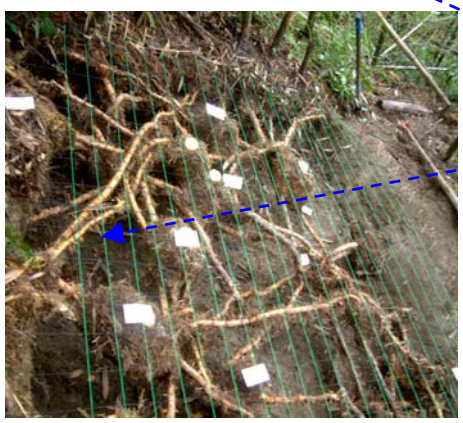

(b) After culms cutting

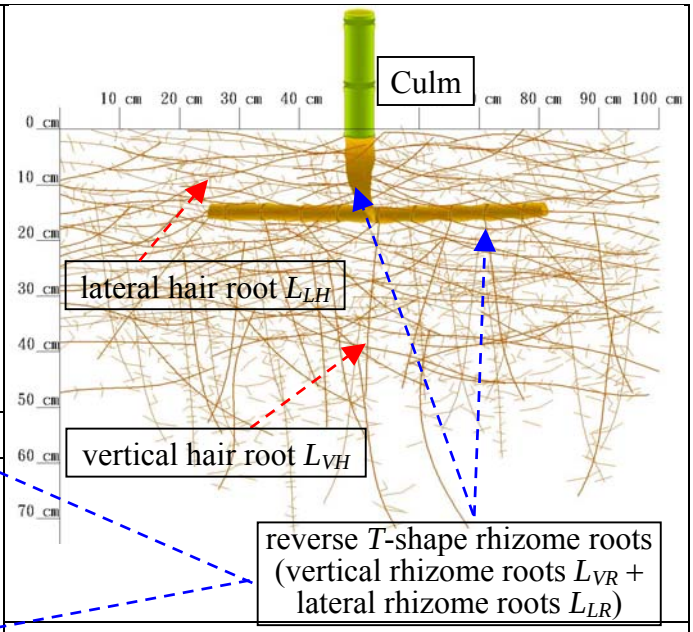

(c) Side view of soil/root system

The root system has a highest root density in the rooting depth of 0 ~ 30 cm due to the growth of large quantity of rhizomes. However, the root density is gradually decreasing in the rooting depth of 30 ~ 60 cm. The root area ratio varies from 0.09 to 0.44% in the rooting depth of 0 ~ 60 cm.

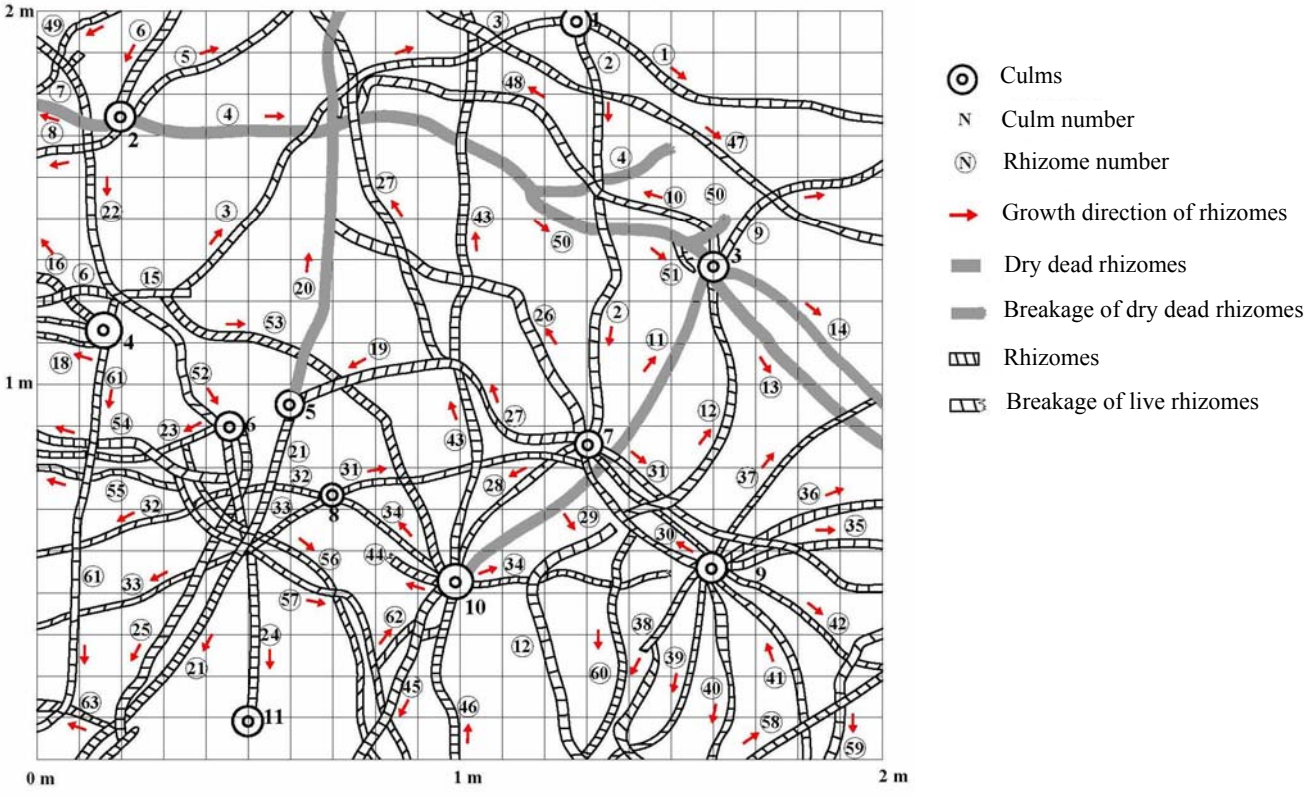

(d) Illustrative sketch of rhizome roots

Fig. 3 Makino bamboo root morphology

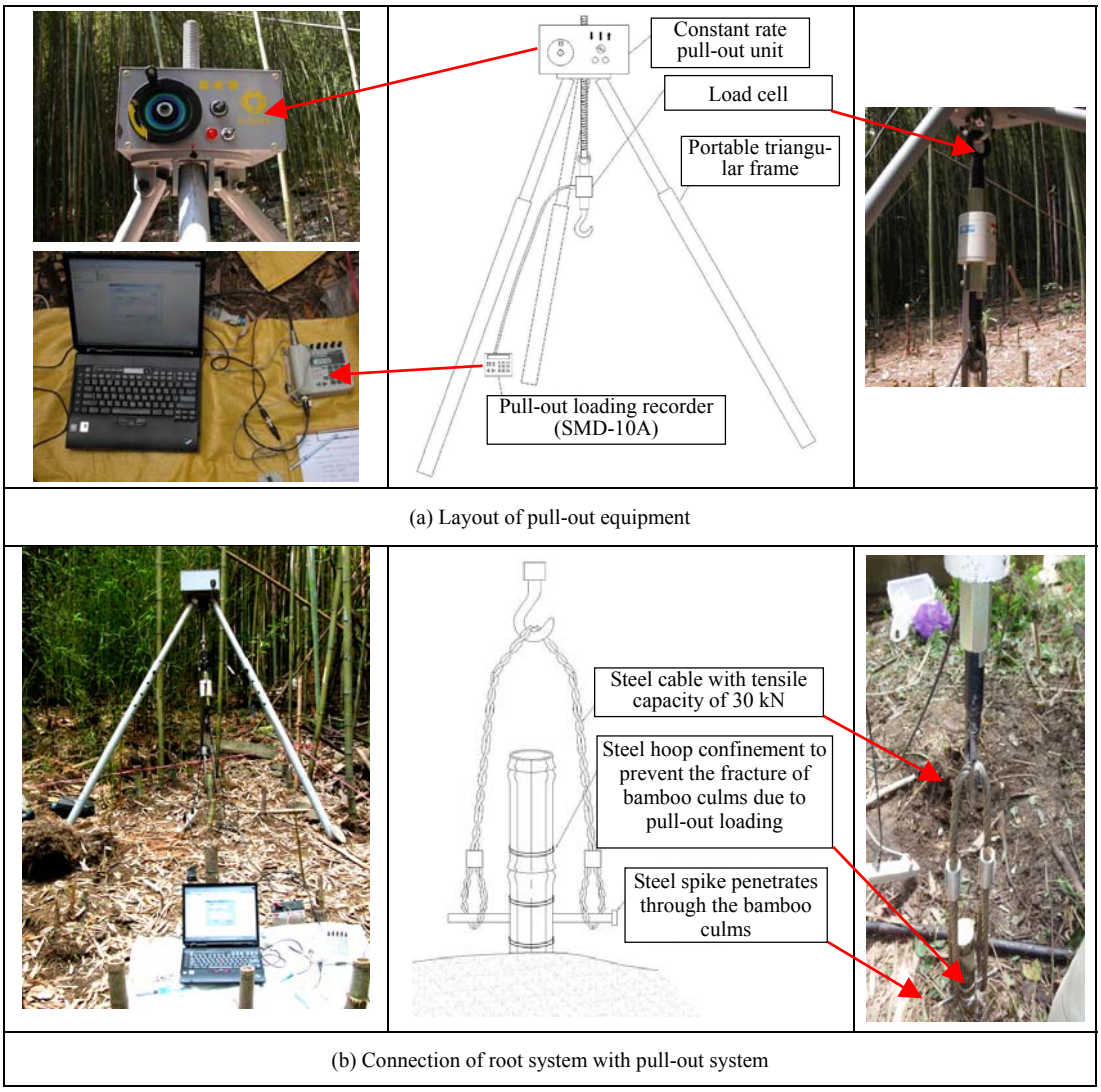

Fig. 4 Pull-out equipment and its connection with Makino bamboo root system

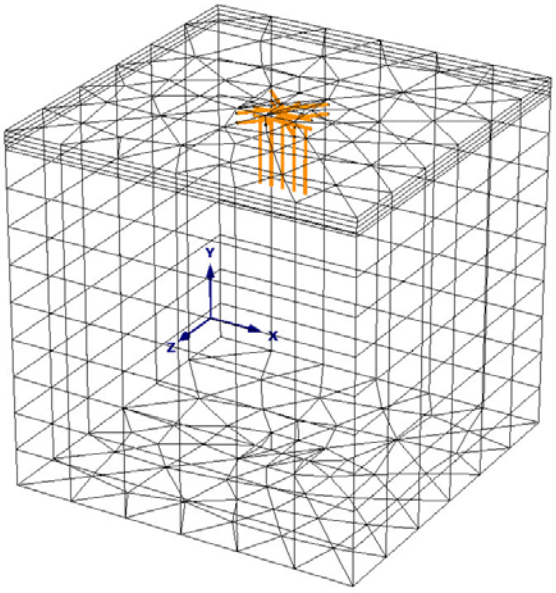

Fig. 5 Numerical model for the pull-out test of Makino bamboo soil-root system

Table 3 Makino bamboo numerical root models and numerical results of pull-out tests

Numerical Root Sample No.	Reverse *T*-shape rhizome root	Vertical hair root	Lateral hair root	δ_p (mm)	P_u (kN)
*S*1	yes	no	no	176	6.082
*S*2*	yes	L_{VH} = 0.50 m	L_{LH} = 0.35 m; 3-layers	178	5.396
*S*3	yes	L_{VH} = 0.50 m	L_{LH} = 0.25 m; 3-layers	199	4.905
*S*4	yes	L_{VH} = 0.50 m	L_{LH} = 0.25 m; 2-layers	206	4.709

yes = with configuration, no = without configuration

L_{VH} = length of vertical hair root; L_{LH} = length of lateral hair root

δ_p = simulated pull-out displacement at ultimate pull-out resistance; P_u = simulated ultimate pull-out resistance

* Due to the similarity of the numerical outputs of 3-D pull-out tests, only *S*2 was used for discussions.

Table 4 Material model parameters of root system for the numerical simulation of pull-out test and direct shear test of Makino bamboo soil-root system

Root system	Root Diameter d (mm)	Cross sectional area a (mm^2)	Ultimate tensile resistance t (kN)
Rhizome root	19.0	283.5	6.81
Hair root	1.5	1.8	3.93
Young's modulus E_r = 312 kPa for root system			

The root material was simulated by a 3-node beam element with a linear elastic model as listed in Table 4. Based on the laboratory tensile test of single root, the ultimate tensile resistance of single root t was determined by $0.0173 \times d^{2.03}$ (d = root diameter) of 6.82 kN and 0.04 kN for rhizome root diameter d_R = 19 mm and hair root diameter d_H = 1.5 mm respectively. In addition, the average Young's modulus of root material E_r = 312 kPa from tensile test was used for the numerical simulation.

Numerical Simulation of Pull-out Test

The simulation of the pull-out test was implemented by continuously applying an incremental pull-out loading to the root system and recording the calculated pull-out displacement increment. The simulation was ceased as the cumulative loading reached the ultimate pull-out resistance P_u of the test curve.

2.7 Numerical Model of Direct Shear Test

As shown in Fig. 7, the dimensions of the numerical model were 3 × 3 × 3 m (= length × width × height) and the central testing block of the soil-root system was 0.60 × 0.6 × 0.15 m (= length × width × thickness). The numerical model with dimension similar to the pull-out test was considered to minimize the boundary effect on the central testing block (direct shear test). The numerical modeling of direct shear test with applied shear loading was performed on the central testing block only. The trench surrounding the testing block was excavated to a depth of 0.15 m to simulate the space required for equipment installation. The shearing plane was specified at a depth of 0.15 m which exactly coincided with the elevation of the intersection point of the vertical and lateral rhizome roots (or reverse T-shape rhizome roots) as indicated in Fig. 6 (see Front View). The outermost geometric boundaries of the numerical model were assumed to be constrained without displacement.

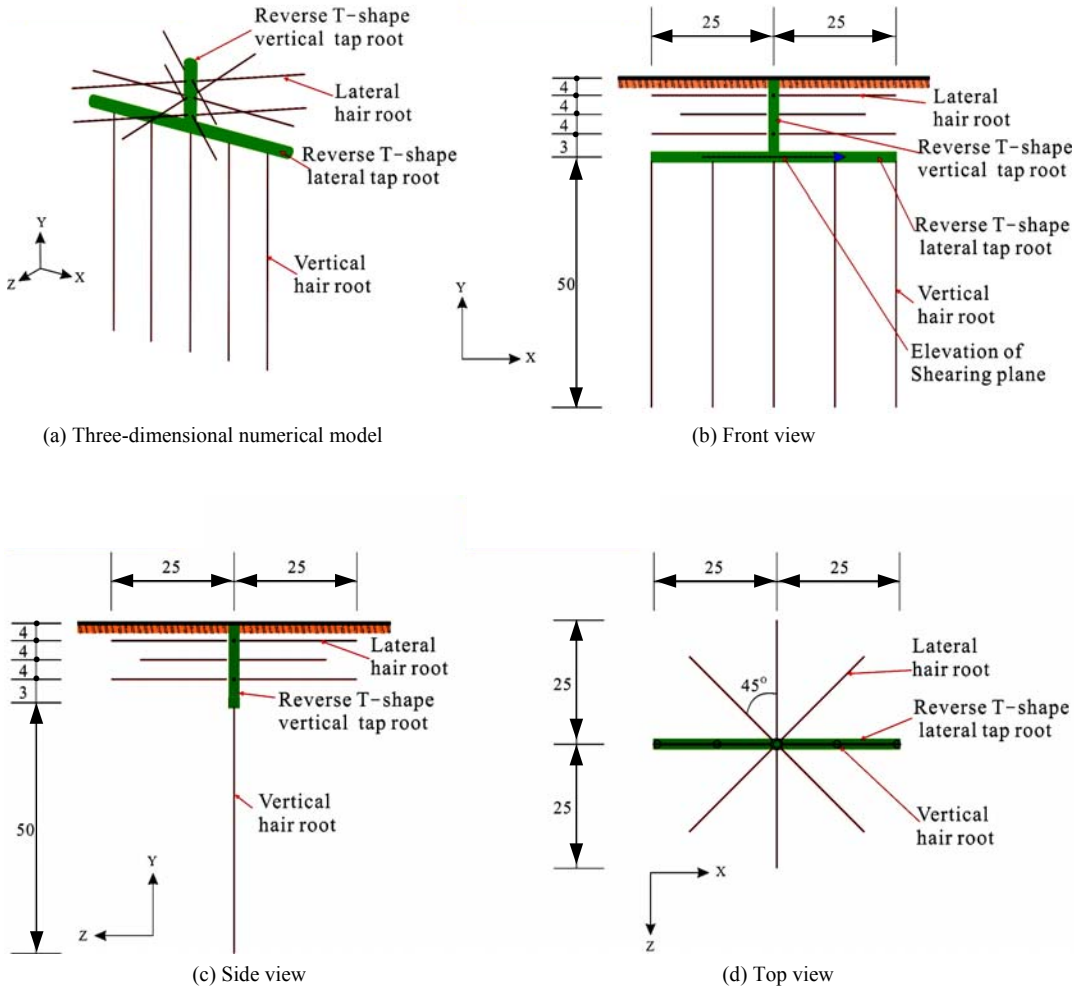

(a) Three-dimensional numerical model

(b) Front view

(c) Side view

(d) Top view

Fig. 6 3-D numerical root model (tap root = rhizome root) of Makino bamboo root system (Unit: cm)

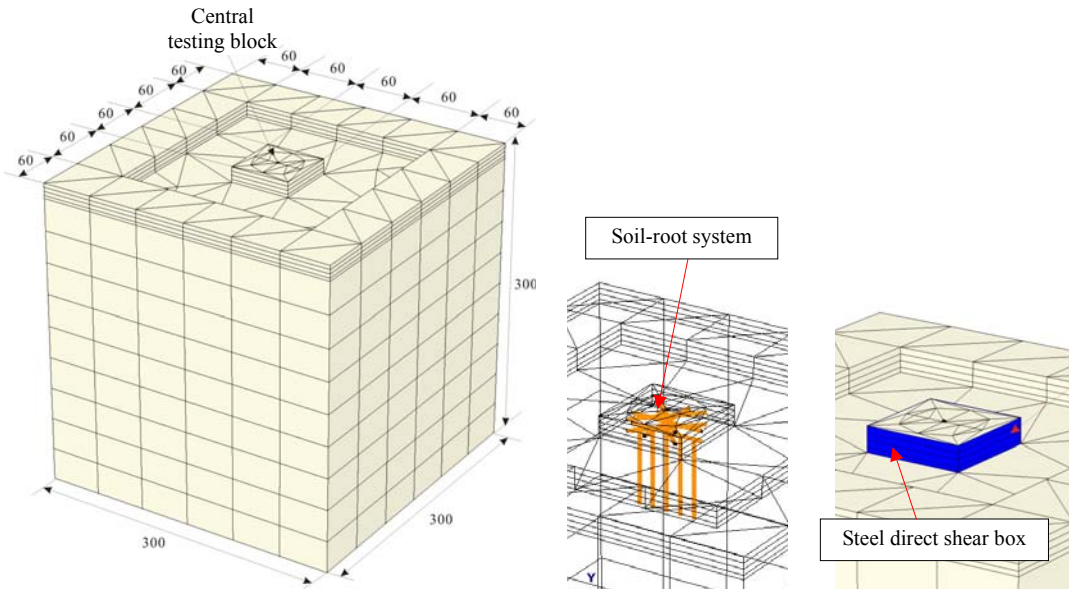

Fig. 7 Numerical model for the direct shear test of Makino bamboo soil-root system (Unit: cm)

Input Material Model Parameters of Direct Shear Test

Except for the strength parameters, the soil *No-B* which possesses a set of input material model parameters of Mohr-Coulomb model similar to the soil *No-A* was used for the numerical simulation of direct shear test. The soil *No-B* has higher strength parameters of cohesion, c = 25 kPa, and friction angle, $\phi = 30°$, than those of the soil *No-A* (c = 24.0 kPa and $\phi = 15.6°$).

The root material parameters were the same as those of the pull-out test (see Table 4). In general, for the in-situ direct shear test of a soil-root block, the loading from hydraulic jack is applied on the sample block through a steel plate. To simulate the shear behavior of the sample block as close as possible, it is suggested to add the shear box with Young's modulus of steel to the model. As shown in Fig. 7, the direct shear box of the steel plate was simulated by a wall element with a linear elastic model and the typical values of material parameters can be given as follows: Young's modulus E_s = 200 GPa, unit weight γ_s = 78.5 kN/m^3, and Poisson's ratio ν_s = 0.29.

Numerical Simulation of Direct Shear Test

In total, three groups of numerical simulations were performed on the direct shear test of Makino bamboo soil-root system, namely, *S*2, *S*3 and *S*4. Similar to the laboratory direct shear test of soil material without roots, the normal stress σ on the shearing plane for the four specimens in each group was varied by 2.7, 7.7, 12.7 and 32.7 kPa ($\sigma = \sigma_o + \Delta\sigma$). In which, the overburden stress σ_o = 0.15 m × 18 kN/m^3 = 2.7 kPa and the normal stress increment was $\Delta\sigma$ = 0, 5, 10 and 30 kPa respectively. The peak shear strength of soil-root system was determined when a large portion of plastic failure occurs in soil mass and the calculation will terminate simultaneously.

2.8 Stability Analyses of Makino Bamboo Forest Slopeland

In summary, the reinforcement effect of the root system on the slope stability was considered by adding a group of root inclusions into the soil mass or using an equivalent reinforced layer with shear strength increment ΔS_r (or cohesion increment of Δc) to represent the soil-root layer (Waldron 1977; Wu *et al*. 1976, 1994, 2004; O'Loughlin and Ziemer 1982; Operstein and Frydman 2002; Lin *et al*. 2007). In addition, Ekanayake *et al*. (1999, 2004) derived the factor of safety of soil with roots at a known shear displacement of direct shear tests using an energy approach. By a simple and practical way, Osman and Barakbah (2006) predicted the slope stability by the parameters of soil water content and root profiles. In conclusion, the main difficulties in evaluating the reinforcement effect of root systems result from the spatial random distribution of the physical and mechanical properties of plant roots. In this study, the soil-root system of Makino Bamboo forest slopeland was modeled by an equivalent reinforced layer with a cohesion increment of Δc.

Numerical Model

The geometry model of Makino Bamboo forest slopeland is displayed in Fig. 8. The slope height of 10 m (= *H*) is maintained while the slope angle β varied from Grade 4 to Grade 7 according to the standard of the slopeland grading system in Taiwan. The grading system gives the following gradations: Grade-4 ($\beta = 20°$, H/L = 36.4%); Grade-5 ($\beta = 25°$, H/L = 46.6%); Grade-6 ($\beta = 40°$, H/L = 83.9%) and Grade-7 ($\beta = 50°$, H/L = 119.2%). The side boundaries and bottom boundaries of the geometric model were restrained without displacement ($\Delta X = 0$; $\Delta Y = 0$; $\Delta Z = 0$).

Input Model Parameters

To evaluate the effect of the Makino bamboo root system on the slope stability, the relative factor of safety, *RFS* (= FS_r / FS_o), proposed by Operstein and Frydman (2002) was used. At first, a critical cohesion c_o was back calculated to maintain the slope without root system at a critical state equilibrium condition for a safety factor FS_o = 1.0. Subsequently, the identical slopes with Makino Bamboo roots were analyzed for a safety factor FS_r. In such a way, the *RFS* enables an evaluation of the exact contribution of the shear strength increment due to roots to slope stability.

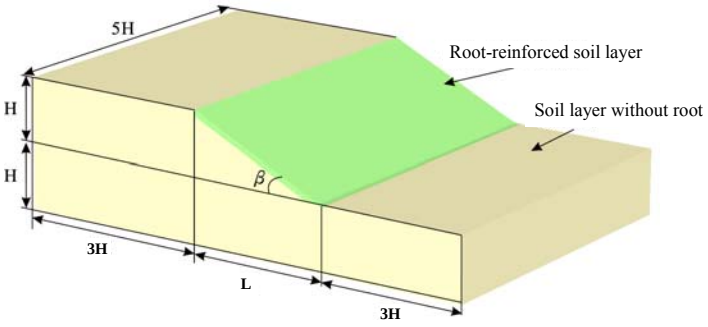

Fig. 8 Geometry dimension (Unit: m) of 3-D numerical model of Makino bamboo forest slopeland

As shown in Table 5, the critical cohesions c_o of 7.47, 8.58, 11.75 and 13.64 kPa can be determined for the slopes with different slope angles β of 20°; 25°; 40° and 50°. The soil material model parameters were same as those of the simulation of direct shear test (the soil *No-B*) and the shear strength increment due to roots Δc = 20.8 kPa (see Table 7) was obtained from the simulations of the direct shear test of the Makino bamboo soil-root system. The soil-root system in the rooting depth L_r = 0.8 m, 0.9 m and 1.0 m were considered as an equivalent reinforced layer with thicknesses of 0.8 m, 0.9 m and 1.0 m and cohesion of c (= c_o + Δc).

Implementation of Stability Analysis

Slope stability analyses were performed on a series of fictitious slopes with and without root systems using the *c*-ϕ reduction method of 3-D finite element program (Plaxis-3D Foundation, 2008). In the *c*-ϕ reduction approach the input strength parameters c (= c_o + Δc) and tanϕ for soil-root system are successively reduced to residual values of c_r and tanϕ$_r$ respectively to trigger the slope failure. The method defined the overall safety factor of slope $FS = (c/c_r) = (\tan\phi / \tan\phi_r)$.

3. RESULTS

3.1 Strengths of In-situ Soil and Single Root

In this study only one type of soil material (soil *No-A*) sampled from the field site was used for the laboratory direct shear test. According to the testing results, the strength parameters (cohesion c and friction angle ϕ) decreased with the increasing water content w. Namely, for w = 7%, 9% and 12%, the corresponding c values and ϕ angles are: c = 43.0 kPa, 39.5 kPa and 24.0 kPa, and ϕ = 24.1°, 19.0° and 15.6°.

According to the testing results, the tensile resistance of a Makino bamboo single rhizome root t can be approximated by t (kN) = [0.0173 × $d^{2.03}$] for the root diameter d (mm) ranging from 13.5 to 23.6 mm by regression fitting procedure. Moreover, the Young's modulus of Makino bamboo rhizome root E_r ranging from 193.3 to 451.3 kPa is equivalent to the secant modulus at the 50% of the maximum tensile stress of the stress/strain curves of tensile tests. The laboratory testing results of rhizome root are summarized in Table 6. It was indicated that the average tensile strength of a live cutting of rhizome root is 20.53 MPa, which is lower than that of dry dead rhizome root at 29.81 MPa and this implies that the dry dead roots can still provide reinforcement to the soil mass. However, it should be noted that the reinforcement effect may be attenuated due to the separation of the dry dead root from the desiccated soil mass. The shear strength of rhizome root was determined by single shear test using universal testing machine.

Table 5 Soil material model parameters for slope stability analyses with and without Makino bamboo root systems

Mohr-Coulomb soil model parameters					
c (kPa)	ϕ (deg.)	γ_{sat} (kN/m^3)	E (kPa)	ν	ψ (deg.)
c_o (Critical cohesion)	30	19.0	2000	0.3	0
Critical cohesion for slopeland with various slope angle					
Slope angle β (deg.) H/L (%) (Slope grade*)	20° 36.4% (Grade-4)	25° 46.6% (Grade-5)	40° 86.9% (Grade-6)	50° 119.2% (Grade-7)	
Critical cohesion c_o (kPa)	7.47	8.58	11.75	13.64	
* In Taiwan, slopeland is classified into Grade-1 ~ Grade-7 according to its slope angle. E = Young's modulus, ν = Poisson's ratio, ψ = dilation angle					

3.2 Verification of Numerical Procedures of the Pull-out Test

Because of the similarity of the numerical outputs of 3-D pull-out analyses, only the simulation results of numerical root sample *S*2 (with reverse *T*-shape rhizome roots, the length of vertical hair root L_{VH} = 0.55 m and 3 layers of lateral hair root with length L_{LH} = 0.35 m) were adopted for discussions. Figure 9 displays the deformation mode of the root system in which the rhizome roots and lateral hair root stretched upward as the pull-out force applied. Nevertheless according to the deformation pattern the vertical hair root seems insignificant in contribution to the pull-out resistance.

Considering the similarity of the pull-out curves, only 4 sets of in-situ pull-out tests (*T*4, *T*5, *T*6 and *T*8) were used for the comparison with the simulations (*S*1, *S*2, *S*3 and *S*4) as shown in Fig. 10. In which, *S*1 ~ *S*4 represents the numerical root samples with different configurations of Makino bamboo root system as listed in Table 3.

The pull-out curves of numerical root samples *S*2, *S*3 and *S*4 exhibited a steeper slope than *S*1 as the pull-out loading was lower than 3 kN at the initial testing stage. This can be attributed to the additional anchorage of the hair roots which extensively scattering over the soil mass surrounding the rhizome roots. However, as the pull-out loading becomes higher than 3 kN, the slope of the pull-out curve of samples *S*2, *S*3 and *S*4 decrease and becomes smaller than *S*1. This can be resulted from the large pull-out displacement of rhizome root and which in turn transferred to the hair roots and its surrounding soil mass in the sequential loading stages. Eventually the anchorage effect of the hair roots descend in response to the failure of surrounding soil mass and leads to a lower ultimate pull-out resistance. In conclusion, except sample *S*1, the simulated pull-out curves of the samples *S*2, *S*3 and *S*4 reasonably fell on the range of measurements.

Table 6 Average tensile and shear strengths of Makino bamboo single rhizome root

Testing Group No.	Root material type	No. of samples tested	Average diameter d (mm)	Average tensile strength σ_t (MPa)	Average shear strength τ_r (MPa)
1	Live cutting	20	20.6 ± 1.32 (σ = 2.83)	20.53 ± 5.06 (σ = 10.85)	non
2	Live cutting	5	19.6 ± 2.51 (σ = 2.19)	non	9.04 ± 5.50 (s = 4.78)
3	Dry dead	5	20.6 ± 2.64 (σ = 2.30)	29.81 ± 11.27 (σ = 9.80)	non

σ: Standard error

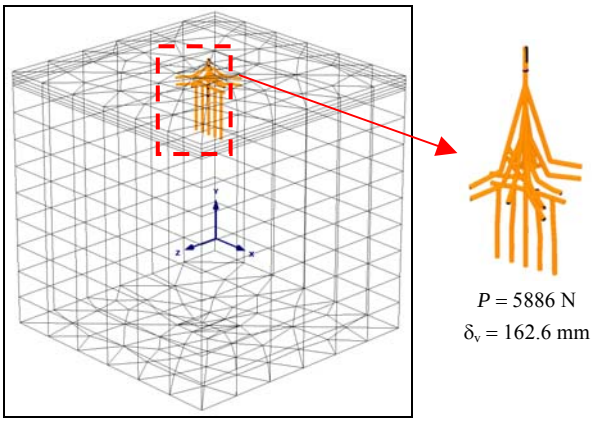

Fig. 9 Deformation mode of Makino bamboo root system S2 at the final loading stage of pull-out test (P = pull-out force, δ_v = pull-out displacement)

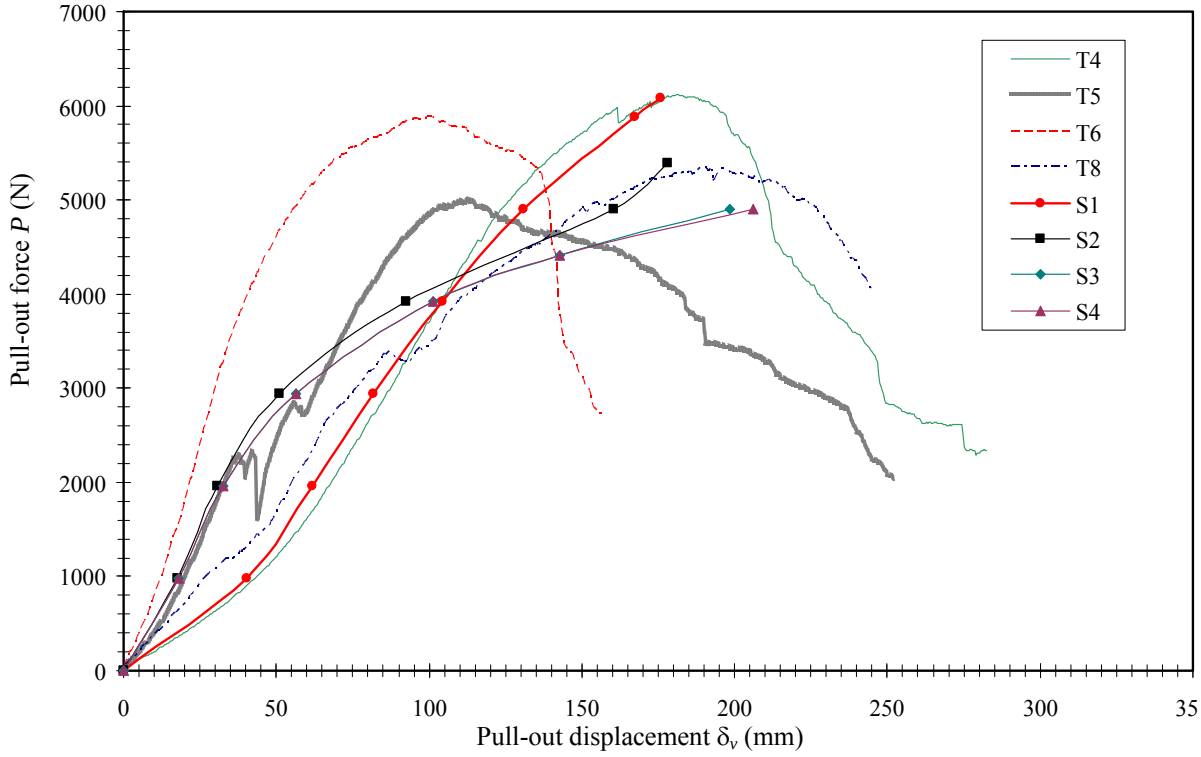

Fig. 10 Comparison between the simulation and measurement of the pull-out test of Makino bamboo soil-root system (T: for Tests and S: for Simulations)

The ultimate pull-out resistance of numerical root samples *S*2, *S*3 and *S*4 shows a sequence of *S*2 > *S*3 > *S*4. Accordingly, for a root system with specific rhizome root morphology, the length (or the extent of lateral spreading) of lateral hair root shows more influence on the anchorage and ultimate pull-out resistance than the number of layer of lateral hair root.

In Fig. 10, the numerical root of type *S*1 which possesses the most simple root pattern (without hair root, see Table 3) displays a distinct simulation curve of pull-out test from those of the numerical roots of type *S*2, *S*3 and *S*4. The pull-out curves of *S*2, *S*3 and *S*4 show a very similar trend from calculations. Accordingly, the numerical root of type *S*1 was excluded from the simulation of direct shear test and only *S*2, *S*3 and *S*4 were considered.

3.3 Numerical Simulations of the Direct Shear Test

Figures 11 present the simulation results of numerical sample *S*3 under various shear loading condition (maximum shear stress τ = 58.9 kPa, maximum shear displacement δ_h = 46.5 mm). A lateral movement of the Makino bamboo root system is mobilized after shearing. Figure 12 shows the Mohr-Coulomb shear strength envelopes of the soil mass with and without Makino

bamboo root system and the envelopes can be expressed by: $\tau = 45.8 + \sigma \times \tan 29.9° = (c + S_r) + \sigma \times \tan 29.9°$ and $\tau = 25 + \sigma \times \tan 30° = c + \sigma \times \tan 30°$. Consequently the shear strength increment due to roots $\Delta S_r = 20.8$ kPa is determined. Table 7 summarizes the ΔS_r (= Δc) determined from the numerical results of direct shear tests *S*2, *S*3 and *S*4.

4. DISCUSSION

4.1 Input Strength Parameters of Soil Model for Different Numerical Simulations

As obtained from the laboratory direct shear tests, the strength parameters of in-situ soil material (c = 43.0 ~ 24.0 kPa, and ϕ = 24.1° ~ 15.6°) decrease with the increasing water content (w = 7 ~ 12%), considering the most conservative condition, the lowest strength parameters (soil *No-A*): c = 24.0 kPa and ϕ = 15.6° with highest water content of 12% were then adopted for the numerical simulation of pull-out tests. It was also found that the numerical calculations of the pull-out curves can be successfully achieved without any numerical difficulty using the lowest strength parameters and compared with the field measurements (see Fig. 10).

However, it should be pointed out that the lowest strength parameters: c = 24.0 kPa and ϕ = 15.6° for the Mohr-Coulomb soil model used in the numerical simulation of direct shear tests will cause numerical difficulties. Due to the low friction angle, the plastic yielding of soil material occurs very fast in the simulation phases and it will automatically cause a termination during the numerical calculations. This consequence is attributed to the difference of the loading type between pull-out test and direct shear test. In pull-out test, the pull-out loading was immediately applied on the root material and then transferred to the surrounding soil mass and this alternately mitigates the occurrence of the plastic yielding of soil. On the contrary, unlike the simulation of pull-out test, in direct shear test, the soil material adjacent to the edge of shear box will carry the shear loading firstly and yield very quickly under a relatively low friction angle prior to the mobilization of the shear resistance from the roots at the central area of shear box. In such circumstances, in order to complete the simulation phases of direct shear test, another set of strength parameters (soil *No-B*) with adjustment of c = 25 kPa and ϕ = 30° was verified to be appropriate for the numerical calculations of direct shear tests. Conclusively, in this study, the soil *No-A* (with lower shear strength parameters) was used for the simulation of pull-out tests whereas the soil *No-B* (with higher shear strength parameters) adopted for the simulation of direct shear test.

4.2 In-situ Pull-out Test

Compared with the lateral uprooting tests by Stokes *et al*. (2007), the maximal lateral pulling force of Big Node bamboo F (= 1615 ± 195 N) which well correlated with the number of roots N (total number of lateral roots=31 and number of roots per node = 5.7) and root volume V_{root} is smaller than the ultimate vertical pull-out resistance P_u (= 5420 ± 470 N) of Makino bamboo. The biomasses of the rhizome roots and the hair roots of Makino bamboo are about 2746.0 kN/ha and 98.1 kN/ha respectively. The difference of the pull-out resistance of the two bamboo

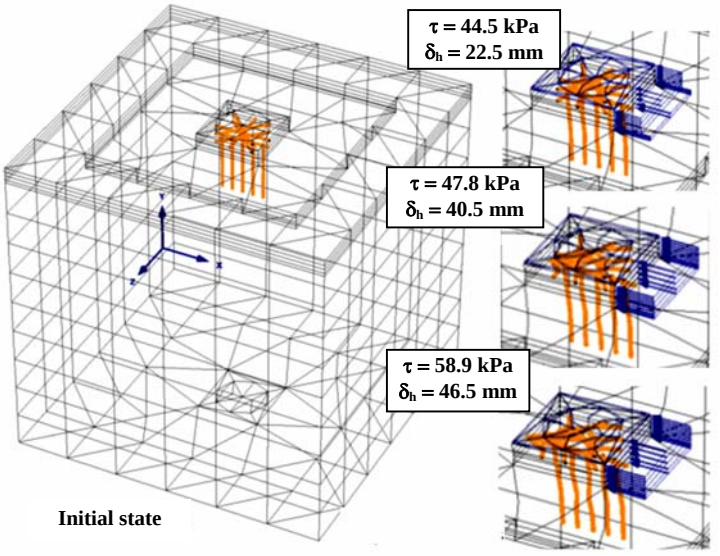

Fig. 11 Deformed mesh of a Makino bamboo soil-root system (*S*3) under different shear loading conditions of direct shear test (τ = shear stress, δ_h = shear displacement)

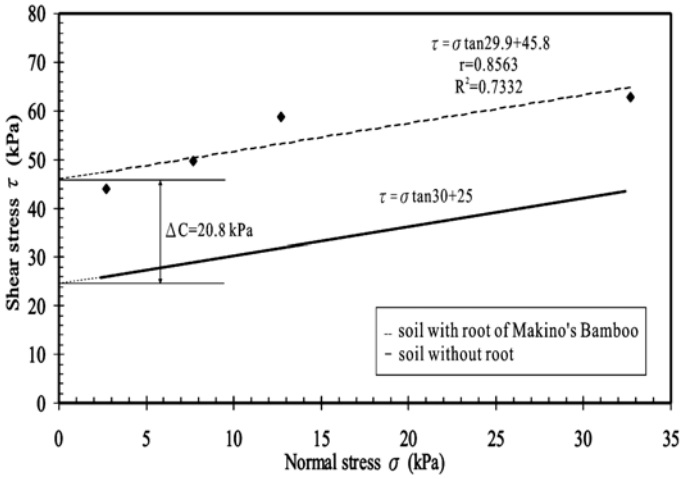

Fig. 12 Shear strength increment due to roots of a Makino bamboo soil-root system (*S*3)

Table 7 Shear strength increment of a Makino bamboo soil-root system determined by numerical simulation of direct shear test

Testing group	c (kPa)	ϕ (deg.) measurement	ϕ (deg.) calculation	$c + \Delta S_r$ (kPa)	ΔS_r (= Δc) (kPa)
*S*2	25	30	29.8	50.3	26.3
*S*3*	25	30	29.9	45.8	20.8
*S*4	25	30	30.1	43.4	18.4

Mohr-Coulomb shear strength envelope of soil mass without root system: $\tau = 24.0 + \sigma \times \tan 30°$
Mohr-Coulomb shear strength envelopes of soil mass with root system: $\tau = 50.3 + \sigma \times \tan 29.8°$ for *S*2; and $\tau = 43.4 + \sigma \times \tan 30.1°$ for *S*4
*The numerical results $\tau = 45.8 + \sigma \times \tan 29.9°$ for *S*3 were used for discussions.

species can be resulted from the differences of the root morphology, the biomass of root system and the loading system of pull-out force (one is lateral uprooting force and another is vertical pull- out loading). Although lacking the exact data of the biomass of root system for comparison, according to the root morphologies surveyed from the field site, the Makino bamboo seems to appear a denser biomass of root system than the Big Node bamboo. In addition, the vertical pull-out resistance of Makino bamboo can be highly mobilized as the root system is fully stretched out at the ultimate state and this pull-out mechanism is different from the lateral uprooting tests carried out by Stokes *et al*. (2007). Nevertheless, it should be emphasized that the lateral uprooting tests pulled plants laterally and downhill near ground level is more representative of failure during a landslide than vertical uprooting.

4.3 Quick Estimation of the Ultimate Pull-out Resistance of Makino Bamboo

In Section 3.2, the ultimate pull-out resistance of Makino bamboo soil-root system is correlated with the diameter at breast height D and the growth age Yr. Considering the non-destructive pull-out testing condition and the soil properties, the ultimate pull-out resistance P_u can be correlated with the growth age Yr, diameter at breast height D and soil water content w as:

$$P_u = 1.61 - 0.03Yr + 0.11 \times D - 0.22 \times w$$
$$(\text{for } Yr = 1 \sim 3 \text{ year},\ D = 35 \sim 70 \text{ mm},\ \text{and } w = 7 \sim 18\%) \quad (1)$$

In practice the Yr, D and, w values are much easier to measure than other parameters in the field site. The above model equation was constructed by the multi-linear regression model. In the model, the co-linearity of Yr, D and, w are evaluated by their *V*ariance *I*nflation *F*actors (*VIF*) and the characteristic of normal distribution of the model was verified by the plots of standard residuals from residual analyses. The *VIF* is used to examine the co-linearity of the regression variables, Yr, D and w. The *VIF* value for each variable can be calculated with respect to the other variables through multi-linear regression analysis. A variable with high *VIF* value ($VIF > 10$) represents the variable has high co-linearity with the other variables and need to be replaced and further examined (Myers, 1986).

4.4 Regression Equation of the Mechanical Conversion Model

The direct shear test of the soil-root system was very tedious and time consuming compared to the pull-out test. To cope with this situation, a mechanical conversion model between the ultimate pull-out resistance and the shear strength increment of the soil-root system due to roots becomes crucial. The model enables a direct transformation of the ultimate pull-out resistance into the shear strength increment of a soil-root system and an immediate application to the stability analyses of Makino bamboo forest slopeland. The shear strength of a soil-root system can be given by: $\tau = (c + \Delta S_r) + \sigma \times \tan\phi$, in which ΔS_r is the shear strength increment contributed by the root system. Using the numerical results of shear strength increment ΔS_r and ultimate pull-out resistance of *S*2, *S*3 and *S*4 as summarized in Table 8, the regression equation for the mechanical conversion model can be expressed by:

Table 8 Numerical results of the shear strength increment due to roots and ultimate pull-out resistance of a Makino bamboo soil-root system

Testing group	Pull-out test			Direct shear test
	P_u (kN)	d (m)	δ_p (m)	ΔS_r (= Δc) (kPa)
*S*2	5.40	0.019	0.178	26.3
*S*3	4.91	0.019	0.199	20.8
*S*4	4.71	0.019	0.206	18.4

d = average diameter of tap root, δ_p = pull-out displacement at ultimate pull-out resistance
Δc = cohesion increment due to roots

$$\Delta S_r = f(P_u) = m \times (P_u)^n = 0.3357 \times (P_u)^{2.5876} \quad (R^2 = 0.999) \quad (2)$$

In which, P_u (kN) = ultimate pull-out resistance of the Makino bamboo soil-root system and m, n = conversion parameters (or regression coefficients). For the Makino bamboo root system, the parameters m and n equal to 0.3357 and 2.5876 respectively.

In fact, the m and n values are the regression coefficients determined by the regression analysis of the shear strength increment ΔS_r and the ultimate pull-out resistance P_u. In this study, the m and n values can not straightforward be correlated with any element of the morphology of the root system. The m value of 0.3357 and n value of 2.5876 are only appropriate for the Makino bamboo root system with the observed ultimate pull-out resistance P_u ranging from 2.28 to 6.12 kN.

For different species of plantation, it needs to determine their own m and n values by the similar operation processes. In practice, the m and n values can be simply determined by two sets of in-situ pull-out tests and in this study the effect of the morphology of a root system can not be directly correlated with the m and n values through the root geometries. However, due to lacking of the actual information of in-situ direct shear test a further verification of the ΔS_r value for Makino bamboo soil-root system is still needed.

The simulated envelopes of direct shear test in Fig. 14 repeatedly verify the validity of previous studies (Wu 1976; Wu *et al.* 1979; Waldron 1977; Waldron and Dakessian 1981) which attributed the shear strength increment of soil-root system ΔS_r to the cohesion increment Δc whereas the frictional angle remains unchanged. Comparatively, O′Loughlin and Ziemer (1982) summarized some typical values from 1 to 17.5 kPa for the increase of soil cohesion Δc due to roots. Wu (1976) derived the shear strength increment of soil-root system due to roots $(\Delta S_r)_{wu}$ considering the roots embedded into the shear zone of a sliding soil mass and obtained $(\Delta S_r)_{wu} = (0.92) \times (\sigma_t) \times (a_r)$ by assuming the root breakage under shearing. In which σ_t = average tensile strength of Makino bamboo root = 20.53 MPa (see Table 6), a_r = area ratio of Makino bamboo root = 0.09 ~ 0.44% (Lin *et al.* 2009), and eventually $(\Delta S_r)_{wu}$ = 17.00 ~ 83.10 kPa. Comparing Wu's shear strength increment $(\Delta S_r)_{wu}$ with that from this study ΔS_r (= 18.4 ~ 26.3 kPa) in Table 8, Wu's mechanical model seems only appropriate for the prediction of shear strength increment of Makino bamboo soil-root system with lower root area

ratio (a_r = 0.10 ~ 0.14%) and root breakage type of failure. However, according to the field observation, the breakage of Makino bamboo roots is seldom or negligible during the pull-out test, consequently, the Wu's mechanical model may overestimate the shear strength increment due to roots in Makino bamboo soil-root system.

4.5 Stability Analysis of Makino Bamboo Forest Slopeland

Makino bamboo has an extremely dense root system and entangles itself with the surrounding soil mass to form a compact soil-root network block of integrity. This is beneficial to the shear strength and the conservation of rainwater. The Makino bamboo rhizome roots are laterally widespread and vertically distributed to form a network texture with high tensile strength which functions as a reinforcement of the foundation soil.

Using the c-ϕ reduction stability analyses, the reinforcement effect of the root system, the sensitivity of rooting depth L_r (= 0.8, 0.9 and 1.0 m) and the slope angle β (= 20°, 25°, 40° and 50°) of Makino Bamboo forest slopeland were investigated. Figure 13 displays the potential sliding mode of Makino Bamboo forest slopeland with rooting depth of L_r = 1.0 m and varied slope angles. It can be observed that the influence of reinforced layer of root system on the factor of safety was insignificant. The colorful legend represents the total displacement increments at slope failure which do not have a physical meaning, but give an indication of the most likely failure mechanism.

As listed in Table 9, the maximum *RFS* is 1.046 (increment of factor of safety due to roots ΔFS = 4.6%) for the case of β = 40° (H/L = 83.9%, Grade-6, L_r = 1.0 m) and this indicates the influence of the Makino bamboo root system on the stability of slopeland is very limited from the viewpoint of engineering mechanics. For a mild slopeland (β < 25°) the Makino Bamboo root system merely plays a minor role on the slope stability. For a medium slopeland (25°< β <40°), the influences of reinforcement (increasing *RFS*) and rooting depth (variation of L_r) of the root system on slope stability become apparent. Similar to the mild slopeland, in a steep slopeland (β > 40°) the increasing stability of the slope due to roots seems negligible when compared with the large driving force from gravity. In conclusions, the contribution of the Makino Bamboo root system has little effect on the stability of slopeland and this is coincides with that of Big Node bamboo indicated by Stokes *et al*. (2007). They concluded that the root system of Big Node bamboo with very shallow rooting depth is probably less useful in preventing soil mass movement and contributes little to slope stability.

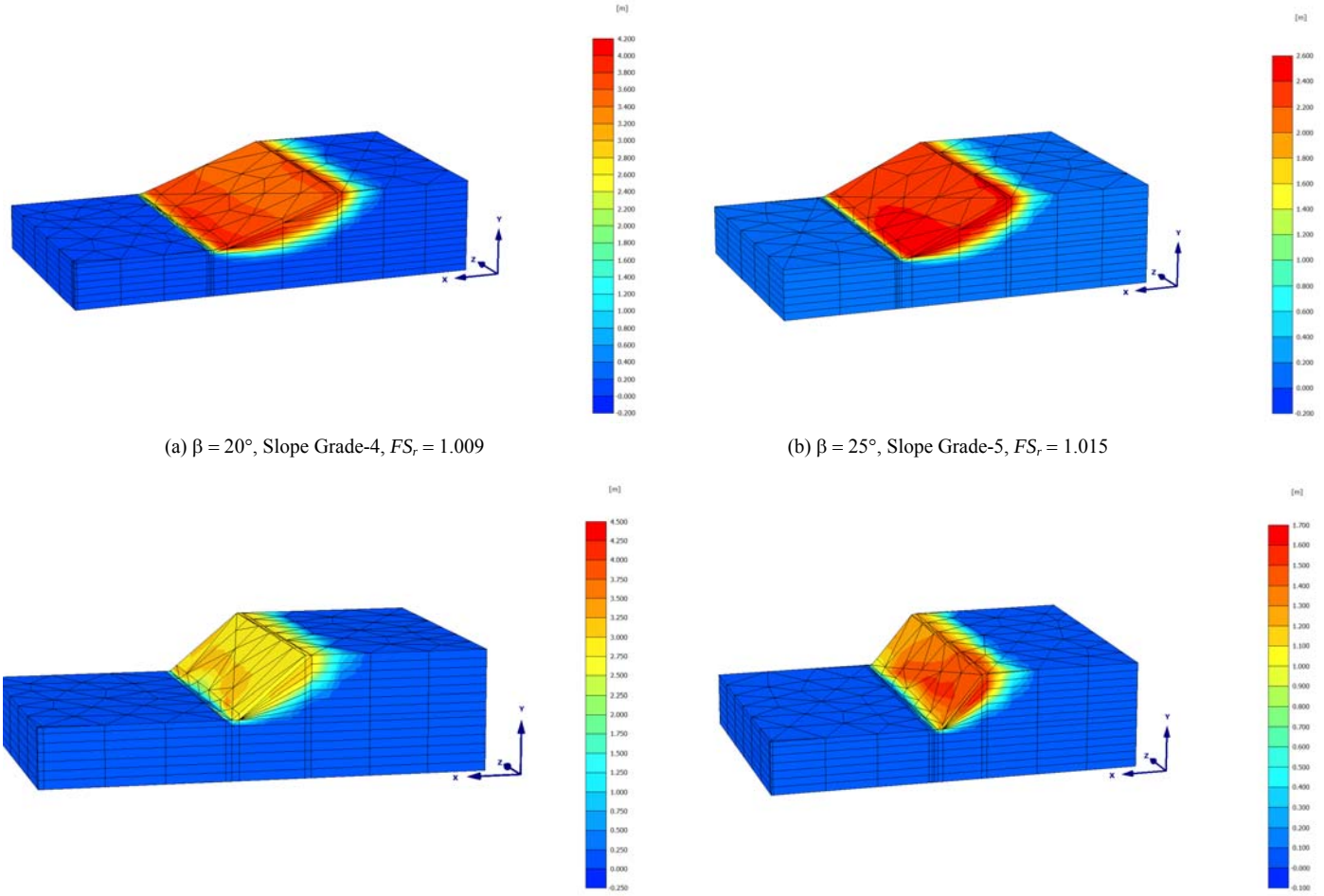

(a) β = 20°, Slope Grade-4, FS_r = 1.009

(b) β = 25°, Slope Grade-5, FS_r = 1.015

(c) β = 40°, Slope Gade-6, FS_r = 1.046

(d) β = 50°, Slope Grade-7, FS_r = 1.025

Fig. 13 Potential sliding modes and contours of total displacement increment of earth slope at failure with a Makino bamboo soil-root system

Table 9 Relative factor of safety (RFS) of Makino bamboo forest slopeland

Slope angle β (°) Slope gradient *H*/*L* (%) (Grade-No)	Root distribution depth L_r (m)	Relative factor of safety *RFS* (Δ*FS*%)
20 36.4 (Grade-4)	0.8	1.005 (0.5%)
	0.9	1.005 (0.5%)
	1.0	1.009 (0.9%)
25 46.6 (Grade-5)	0.8	1.013 (1.3%)
	0.9	1.014 (1.4%)
	1.0	1.015 (1.5%)
40 83.9 (Grade-6)	0.8	1.033 (3.3%)
	0.9	1.042 (4.2%)
	1.0	1.046 (4.6%)
50 119.2 (Grade-7)	0.8	1.017 (1.7%)
	0.9	1.019 (1.9%)
	1.0	1.025 (2.5%)
Increment of factor of safety due to roots $\Delta FS(\%) = (FS_r - FS_o) \times 100\% / FS_o$ and $FS_o = 1.0$		

4.6 Adverse Influence Factors on the Stability of Makino Bamboo Forest Slopeland

Coppin and Richards (1990) indicated that although the surcharge effect was considered as an adverse effect in the case of trees, surcharge can also be beneficial, depending on slope geometry, the distribution of vegetation over the slope, and the soil properties. However, Gray and Megahan (1981) presented that the surcharge of trees is beneficial only when slope angles are small and this implied an extremely adverse situation to the Makino bamboo forest slopeland which is generally steep with a slope angle of 50° ~ 70° as shown in Fig. 1. Meanwhile, Wu (1979) estimated that the weight of the trees can reach about 5.2 kPa from the number of trees per unit area and their sizes as determined from the survey.

In addition, Coppin and Richards (1990) also demonstrated that wind loading becomes significant when the wind velocity is higher than 11 m/sec and both the up- or down-hill wind loadings can destabilize the slope especially in larger trees with shallow root systems. In 2004, Typhoons Mindulle (02, July; wind velocity = 30 ~ 38 m/sec; rainfall intensity = 267.5 ~ 265.5 mm/day) and Aere (25, August; wind velocity = 38 ~ 48 m/sec; rainfall intensity = 151.5 mm/day) invaded Taiwan and caused severe collapse failure and erosion of Makino bamboo forest slopeland. In such circumstances, the shallow rooting depth of 0.8 ~ 1.0 m and large growth height over 10 m of Makino bamboo culms became extremely unfavorable to the slope stability.

Tension cracks were also widespread over the slopeland after the typhoons as shown in Fig. 14. It is then speculated that the wind loading induced overturning moment on bamboo culms can be responsible for the tension cracks and the collapse failure of slopeland eventually triggered by the subsequent infiltration of rainwater into the cracks during the torrential rainfall of typhoons.

5. CONCLUSIONS

According to the field investigations and numerical calculations of the Makino bamboo soil-root system, several conclusions were made as follows:

Based on the field surveys of root morphology, a 3-D numerical model of the soil-root system was developed and successfully applied to the simulation of in-situ pull-out behavior. The model simply consisted of a reverse *T*-shape rhizome roots and a limited number of hair roots. The numerical results revealed that the pull-out loading was mainly carried by the tap root whereas the hair roots only play a minor role in providing the pull-out resistance.

(a) Tension cracks at the upper slope of Makino bamboo forest slopeland (b) Tension cracks caused by the bending of Makino bamboo culm

Fig. 14 Tension cracks on the Makino bamboo forest slopeland after typhoons

In practice, the ultimate pull-out resistance P_u for a non- destructive pull-out testing condition was well correlated with the growth age Yr, diameter at breast height D and soil water content w by a regression equation as: $P_u = 1.61 - 0.03Yr + 0.11 \times D - 0.22 \times w$, (for $Yr = 1 \sim 3$ year, $D = 35 \sim 70$ mm, and $w = 7 \sim 18\%$).

Through a series of numerical simulations of the direct shear test, a mechanical conversion model with simple mathematical form, $\Delta S_r = f(P_u) = m \times (P_u)^n = 0.3357 \times (P_u)^{2.5876}$, enabling a direct transformation of the ultimate pull-out resistance P_u (kN) into the shear strength increment of the Makino bamboo soil-root system ΔS_r(kPa) was proposed. The above mechanical conversion equation is effective for the P_u field measurement of 2.28 ~ 6.12 kN for the ΔS_r (= Δc) estimation of 2.83 ~ 36.45 kPa.

The slope stability results indicate the contribution of the soil-root system has little effect on the stability of Makino bamboo slopeland from the viewpoint of engineering mechanics. The increasing stability of the slopeland due to roots seems negligible when compared with several adverse influence factors during typhoons such as the surcharge effect of plants; wind loading induced overturning moment; tension cracks and infiltrating rainwater.

REFERENCES

Abe, K. (1991). "Estimation of reinforced shear resistance of rooted soil by pull-out resistance of the roots." *Journal of Japanese Society Revegetation Technology*. **16**(4), 37–45.

Abe, K. and Ziemer, R. R. (1991). "Effect of tree roots on a shear zone: Modeling reinforced shear strength." *Can. J. For. Res*. **21**, 1012-1019.

Cazzuffi, D. and Crippa, E. (2005). "Shear strength behavior of cohesive soils reinforced with vegetation." *16th International Conference on Soil Mechanics and Geotechnical Engineering*, OSAKA, Japan, September 12~16, 2493~2498.

Coppin, N. J. and Richards, I. G. (1990). "Use of vegetation in civil engineering." Construction Industry, *Research and Information Association* (CIRIA), U.K.

Chen, T. H., Wang, D. X., and Lin, S. H. (2005). "Growth characteristics of bamboo and its potential role in anti-disaster function." *Proceeding of Taiwan-Japan Joint Conference on Natural Hazard Prevention and Vegetation Method*, National Chung-Hsing University, Taichung, Taiwan, March, **22**, 127–136.

Dupuy, L., Fourcaud, T., Stokes, A., and Danjon, F. (2005a). "A density-based approach for the modelling of root architecture: application to maritime pine (pinus pinaster ait.) root systems." *Journal of Theoretical Biology*, **236**, 323–334.

Dupuy, L., Fourcaud, T., and Stokes, A. (2005b). "A numerical investigation into factors affecting the anchorage of roots in tension." *European Journal of Soil Science*, **56**, 319–327.

Dupuy, L., Fourcaud, T., and Stokes, A. (2005c). "A numerical investigation into the influence of soil type and root architecture on tree anchorage." *Plant and Soil*., **278**, 119–134.

Dupuy, L., Fourcaud, T., Lac, P., and Stokes, A. (2007). "A generic 3D finite element model of tree anchorage integrating soil mechanics and real root system architecture." *American Journal of Botany*, **94**, 1506–1514.

Ekanayake, J. C. and Phillips, C.J. (1999). "A method for stability analysis of vegetated hillslopes: An energy approach." *Can. Geotech. J.* **36**, 1172–1184.

Ekanayake, J. C., Phillips, C. J., and Marden, M. (2004). "A comparison of methods for stability analysis of vegetated slopes." *Ground and Water Bioengineering for Erosion Control and Slope Stabilization*, Science Publisher, Inc., 171–181.

Ennos, A. R. (1990). "The anchorage of leek seedlings: The effect of root length and soil strength." *Annals of Botany*, **65**, 409–416.

Ennos, A. R. (1991). "The mechanics of anchorage in wheat triticum aestivum L. II. anchorage of mature wheat against lodging." *Journal of Experimental Botany*, **42**(245), 1607–1613.

Gray, D. H. and Megahan, W. F. (1981). "Forest vegetation removal and slope stability in the Idaho Batholith." Research paper INT-271, Intermoutain Forest and Range Experiment Station, Ogden, Utah.

Gray, D. H. and Sotir, R. B. (1996). "Biotechnical and soil bioengineering slope stabilization. A practical guide for erosion control." *A Wiley-Interscience Publication*, John Wiley and Sons, Inc.

Lee, J. X. (1983). "The growth characteristics of Makino bamboo." *Quarterly Journal of Scientific Evolution*, **11**(9), 861–867 (in Chinese).

Lin, Der-Guey, Huang, Bor-Shun, and Lin, Shin-Hwei (2007). "Quantitative evaluation on the stability of vegetated slope using the equivalent single taproot model." *Journal of Chinese Soil and Water Conservation*, **38**(1), 15–29 (in Chinese).

Lin, S. H., Lin, D. G., and Chen, T. H. (2009). "The growth characteristics and landslide potential of Makino bamboo forest." *Journal of Engineering Environment*, **23**, 25–40 (in Chinese).

Liu, Y. C. and Ren, Y. A. (1971). "A study on the growth environment and growth characteristics of bamboo forest in Taiwan." *Quarterly Journal of Chinese Forestry*, **5**(1), 18–28 (in Chinese).

Morgan, R. P. C. and Rickson, R. J. (1995). "Slope stabilization and erosion control-A bioengineering approach." *E & FN SPON*, London.

Myers Raymond, H. (1986). "Classical and modern regression with applications, 2nd Ed." *Virginia Polytechnic Institute and State University*, Publisher: Duxbury.

O'Loughlin, C. and Ziemer, R. R. (1982). "The importance of root strength and deterioration rates upon EDAPHIC stability in steepland forests." I.U.F.R.O. Workshop P.1.07-00 *Ecology of Subalpine Ecosystems as a Key to Management*. 2-3 August 1982, Corvallis, Oregon. Oregon State University, 70–78.

Plaxis 3D Foundation V2.2, (2008). "Manual of finite element code for soil and rock analyses."

Operstein, V. and Frydman, S. (2000). "The influence of vegetation on soil strength." *Ground Improvement*, **4**(2), 81–89.

Operstrin, V. and Frydman, S. (2001). "Numerical simulation of direct shear of root-reinforced soil." *Ground Improvement*, **5**, 163–168.

Operstrin, V. and Frydman, S. (2002). "The stability of soil slopes stabilised with vegetation." *Ground Improvement*, **6**, 163–168.

Osman, N. and Barakbah, S. S. (2006). "Parameters to predict slope stability-soil water and root profiles." *Ecological Engineering*, **28**, 90–95

Stokes, A., Ball, J., Fitter, A. H., Brain, P., and Coutts, M.P. (1996). "An experimental investigation of resistance of model root systems to uprooting." *Annals of Botany*, **78**, 415–421.

Stokes, A., Lucas, A., and Jouneau, L. (2007). "Plant biomechanical strategies in response to frequent disturbance: Uprooting of

phyllostachys nidularia (Poaceae) growing on landslide prone slopes in Sichuan, China." *American Journal of Botany*, **94**, 1129–1136

Waldron, L. J. (1977). "The shear resistance of root-permeated homogeneous and stratified soil." *Soil Science Society American Journal*, 843–849.

Waldron, L. J. and Dakessian, S. (1981). "Soil reinforcement by roots: Calculation of increased soil shear resistance from root properties." *Soil Science*, **132**(6), 427–435.

Wu, T. H. (1976). "Investigation of landslides on prince of wales island alaska." *Geotechnical Engineering Report No. 5*, Department civil engineering Ohio state university, Columbus, 94P

Wu, T. H., McKinnell, W. P. III, and Swanston, D. N. (1979). "Strength of tree roots and landslides on Prince of Wales Island. Alaska." *Can. Geotech. J.* **16**, 19–33.

Wu, T. H., McOmber, R. M., Erb, R. T., and Beal, P. E. (1988a). "Study of soil-root interaction." *J. of Geotechnical Engineering*, 114(12), 1351–1375.

Wu, T. H., Beal, P. E., Lan, C. (1988b). "In-situ shear test of soil-root systems." *J. of Geotechnical Engineering*, **114**(12), 1376–1394.

Wu, T. H. (1994). "Slope stabilization using vegetation." *Geotechnical Engineering Emerging Trends in Design and Practice*, 377–402.

Wu, T. H., Watson, A. J., and El-Khouly, M. A. (2004). "Soil-root interaction and slope stability ground and water bioengineering for erosion control and slope stabilization." *Science Publisher*, Inc., 183–192.

Yang, Y. C. and Huang, Y. T. (1981). "Management and distribution system of the main commercial bamboo species in the Chu-Shan area of Taiwan." *Quarterly Journal of Chinese Forestry*, **14**(4), 1–28 (in Chinese).